

**Effect of pH on the Langmuir monolayers of Nickel stearate  
and the synthesised Nickel oxide thin films**

*A dissertation submitted*

*in the partial fulfilment of the requirements*

*for the degree of*

**MASTER OF SCIENCE**

in

**PHYSICS**

by

**Amanpreet Kaur**

(301504002)



Under the guidance of

**Dr. Loveleen Kaur Brar**

**Assistant Professor**

**School of Physics and Materials Science**

**Thapar University, Patiala- 147004, INDIA**

**July 2017**

### Declaration

I hereby declare that the project report entitled "**Effect of pH on the Langmuir monolayers of Nickel stearate and the synthesised Nickel oxide thin films**" is the work carried out by me under the supervision of **Dr. Loveleen Kaur Brar**. I have not submitted this work anywhere in other University or Institution for the award of any degree.

Place: *Thapar University, Patiala*

Date: *17/8/2017*

*Amanpreet*  
*17/8/2017*

**Amanpreet Kaur**

### Certificate

This is to certify that project report entitled "**Effect of pH on the Langmuir monolayers of Nickel stearate and the synthesised Nickel oxide thin films**" submitted by **Ms. Amanpreet Kaur** is in partial fulfilment for degree of Master of Science in Physics in this University. This work has been done under my supervision. She has not submitted this work to any University or Institution for the award of any degree.

  
**Dr. Loveleen Kaur Brar**

Assitant Professor

School of Physics and Materials Science

Thapar University, Patiala

*Dedicated  
to my  
Family  
and  
Friends  
for their love.*

## Acknowledgement

With immense pleasure, I am really thankful to my supervisor **Dr. Loveleen Kaur Brar**, School of Physics and Material Science (SPMS), Thapar University, Patiala. Without her dedicated supervision, it would not have been possible for me to complete my thesis work. She always encouraged me whenever I felt down and motivated me to work harder. She was the one who motivated me to go for the work of my interest and every time I went to her with any kind of query she was always there for me.

I wish to express my sincere thanks to **Dr. Manoj Kumar Sharma**, Head of SPMS department for his support and encouragement.

A special thanks to **Ms. Palvi** and **Ms. Rajni Sharma** for their valuable guidance in learning technique. I would like to thank **SAI Labs Thapar University, SAIF Punjab University Chandigarh** and **CIL Central University Bathinda** for doing characterization techniques.

I am thankful to my friend **Rajpal Kour**, for helping me in my characterization techniques.

I am glad to thank my friends **Raveena, Yashjeet Kaur, Navneet Kaur** and **Priyanka** for always motivating me to work harder and to move on with a positive spirit.

Last but not the least, I place a deep sense of gratitude to my Grandfather **Sh. Joginder Singh and my family** for their sincere encouragement, being a source of inspiration throughout my thesis. Their blessings and love means a lot to me and inspires me pursue my work with full enthusiasm and great confidence.

*Amanpreet*  
17/8/2017  
**Amanpreet Kaur**

## **ABSTRACT:**

NiO is an attractive transition metal oxide in regard of its optical, electrical, structural, mechanical and magnetic properties. Nickel oxide thin films find important applications in varied fields such as photovoltaic devices, smart windows, as counter electrode, electrochromic coating etc. So their formation and its control is an important topic of research. Langmuir Blodgett (LB) thin film deposition method is known for the precise control of thin film parameters. In this work the thin uniform films of nickel oxide were synthesized from the Ni-stearate LB films. Stable and compact Langmuir monolayers are the first step in LB film deposition. Their characteristics decide the quality of LB films and the morphology of the final phase formation. Ni-stearate Langmuir monolayers were deposited and characterized on the surface of the Langmuir trough. It was observed that as the concentration and pH of subphase increased the compaction of the film and its static elasticity in the solid phase increased indicating an increase in Ni<sup>2+</sup> ion incorporation. An important result to emerge from these studies was that for very high pH (8.3) the structure of the films opens up. Analysis of  $\pi$ -A isotherms indicated that pH 7.9 had good parameters for the LB deposition. The oscillating barrier characterizations of Ni stearate monolayers at different frequencies and pH values were recorded. It also confirmed the stability of the monolayers at pH 7.9. Transparent Nickel oxide thin films on glass substrate were synthesized by deposition of 10, 15, 19 layers of Ni-stearate at 7.9 pH followed by drying, removal of stearate chain and calcination. The presence of Ni in thin films was checked by EDS. The synthesized nickel oxide thin film has the band gap of 4.04 eV. The thin films formed by deposition of 15 layers of nickel stearate deposited at pH 7.9 were continuous and uniform. The effect of pH on the final film morphology was determined by depositing 15 layers of Ni stearate for 6.9 and 8.3 pH values. The results showed that these films are non-continuous and have large grain size distribution.

## CONTENTS

<b>CHAPTER 1: INTRODUCTION TO NICKEL OXIDE. ....</b>	<b>1-4</b>
1.1 Introduction. ....	1-1
1.2 Structure of Nickel Oxide. ....	1-1
1.3 General Properties of Nickel Oxide. ....	2-2
1.4 Properties of Nickel Oxide as thin films. ....	2-3
1.5 Applications of Nickel Oxide thin films. ....	3-3
1.6 References. ....	4-4
<b>CHAPTER 2: LITERATURE REVIEW. ....</b>	<b>5-10</b>
2.1 Deposition of NiO thin films by various other techniques. ....	5-6
2.2 Effect of pH on Langmuir monolayer. ....	7-7
2.3 Oscillating Barrier Method. ....	7-8
2.4 Deposition of thin films by Langmuir Blodgett techniques. ....	8-8
2.5 Oxide thin films by Langmuir Blodgett techniques. ....	8-8
2.6 References. ....	9-10
<b>CHAPTER 3: LANGMUIR- BLODGETT TECHNIQUE. ....</b>	<b>11-18</b>
3.1 Introduction. ....	11-11
3.2 Formation of Langmuir Monolayer. ....	11-12
3.3 Pressure-Area Isotherm. ....	12-13
3.4 Deposition Methods. ....	13-14
3.5 Types of Langmuir-Blodgett Deposition. ....	14-15

3.6 Oscillating Barrier Measurement .....	15-16
3.7 Langmuir-Blodgett Technique's Experimental Setup.....	16-17
3.8 Advantages.....	17-17
3.9 Disadvantages.....	17-17
3.10 References. ....	18-18

**CHAPTER 4: MATERIALS AND METHODS ..... 19-24**

4.1 Materials used .....	19-19
4.2 Methods.....	20-21
4.2.1 Cleaning of trough.....	20-20
4.2.2 Cleaning of Substrates.....	20-20
4. 2.4 Preparation of subphase... ..	20-20
4.2.5 Preparation of Langmuir films and Langmuir Blodgett films.....	20-20
4.2.6. Oscillating Barrier Method.....	21-21
4.2.7 Drying and Calcination protocol .....	21-21
4.3 Characterization Techniques.....	21-24
4.3.1 Surface Pressure ( $\pi$ ) - Area (A) Isotherm.....	21-21
4.3.2 Field Emission Scanning Electron Microscopy (FE-SEM) .....	22-23
4.3.3 UV Visible Spectroscopy (UV-Vis)... ..	23-23
4.3.4 XRD .....	24-24
4.4 References. ....	25-25

**CHAPTER 5: RESULTS AND DISCUSSION..... 26-42**

5.1 Surface Pressure ( $\pi$ ) –Area (A) Isotherms.....	26-31
---	-------

5.1.1 Effect of subphase concentration .....	26-27
5.1.2 Effect of pH .....	27-29
5.2 Oscillating Barrier characterization of Ni-stearate monolayers. ....	30-31
5.2.1 Effect of barrier oscillation frequency .....	30-32
5.2.2 Effect of subphase pH.....	32-33
5.3 Nickel Oxide films.....	34-37
5.3.1 Deposition of Ni-stearate Langmuir –Blodgett films.....	34-35
5.3.2 Energy-dispersive X-ray spectroscopy (EDS).....	35-35
5.3.3 XRD.....	36-36
5.3.4 UV-Visible Spectroscopy (UV Vis). ....	36-37
5.3.5 Nickel oxide thin film morphology .....	37-40
5.3.5.1 Effect of number of layers.....	37-39
5.3.5.2 Effect of subphase pH.....	39-40
5.4 References. ....	41-41
<b>CHAPTER 6: CONCLUSIONS AND FUTURE SCOPE.....</b>	<b>42-42</b>
6.1 Conclusion.....	42-42
6.2 Future scope... ..	42-42

## 1.1 Introduction:

Nickel oxide is an attractive transition metal oxide due to its optical, electrical, structural, mechanical and magnetic properties. Stoichiometric NiO is an insulator of resistivity of  $10^{13}\Omega\cdot\text{cm}$ . Its resistivity can be decreased by an increase of  $\text{Ni}^{3+}$  ions resulting the appearance of nickel vacancies in NiO crystals.

NiO thin films have been fabricated by various physical and chemical methods. Thin films obtained from different methods differ in stoichiometry, crystallite size etc. Transparent NiO conducting films have many applications such as in photovoltaic devices.

## 1.2 Structure of Nickel Oxide

NiO has a cubic structure similar to NaCl with lattice constant of 0.4177nm. Nickel ion is surrounded by six oxygen ions and each oxygen ion is surrounded by six nickel ions as shown in figure 1.1. Here big red balls represent oxygen ions and black balls represent nickel ions.

Below Neel temperature  $T_N$  ( $\sim 523\text{K}$ ), NiO has an fcc structure with small rhombohedral distortion. Spin polarization of Ni atoms results an anti-ferromagnetic arrangement in the (111) plane [1].

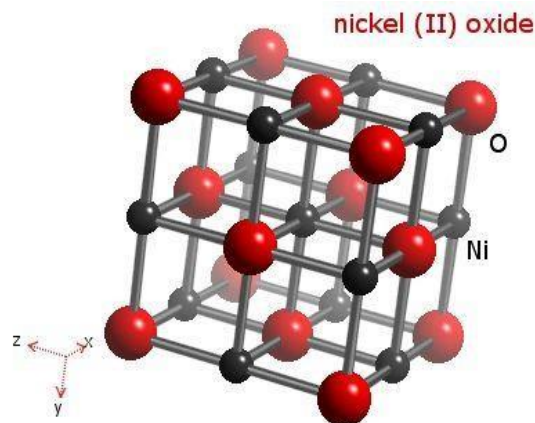


**Figure 1.1** Simple cubic structure of NiO [2]

### 1.3 General Properties of Nickel Oxide

Properties of NiO are as follows:

NAMES	
IUPAC name	Nickel(II) oxide
Other names	Nickelous monoxide
	Oxonickel
PROPERTIES	
Chemical formula	NiO
Molar mass	74.6928 g/mol
Band gap	3.4-4.0 eV
Appearance	green crystalline solid
Crystal structure	Rock salt (octahedral)
Dielectric constant	10
Lattice parameter (a)	4.177Å
Thermal conductivity	91W/(mK)
Hardness	4MPa
Thermal expansion	0.0000134(K <sup>-1</sup> )
Density	6.67 g/cm <sup>3</sup>
Melting point	1995 °C
Refractive index (n <sub>D</sub> )	2.1818
Electron configuration of Ni <sup>2+</sup>	[Ar]3d <sup>10</sup>
Optical density	0.915
Oxide ion polarizability	High
Resistance	10 <sup>-8</sup> (ohm.m)
Elastic modulus	142 to 158GPa

### 1.4 Properties of Nickel Oxide thin films

- **Structural properties:** Structure of NiO thin films depend on oxygen content and deposition method. NiO thin films have polycrystalline structure with

distribution of grains. The grain size of NiO increases with increasing substrate temperature. As thin films thickness increases grain size also increases [2, 3].

- **Electrical properties:** Electrical conductivity of NiO is affected by formation of microstructural defects inside the NiO crystals such as Ni vacancies and interstitial oxygen. In NiO vacancies occur at cation sites due to non-stoichiometry. Thus from one cation vacancy two electrons and holes are formed. These carriers in NiO are cause of variation in electrical conductivity [2].
- **Optical properties:** NiO thin films measured band gap is in between 3.6 eV and 4 eV. Thickness of thin films can be examined by reflectance. As annealing temperature increases transmittance also increases.
- **Mechanical properties:** NiO thin films have low elasticity before heating and after heating above 400 °C elasticity increases due to narrower grain boundaries which is main cause of better elastic behavior. Elastic modulus values for Ni-base super alloy lies in range 142 to 158GPa [4].

## 1.5 Applications of NiO thin films

Applications of NiO thin films are:

- Electrochromic coating
- Resistance switching
- Functional layer materials for gas sensors, such as H<sub>2</sub> sensor.
- p-type transparent conductors
- Photovoltaic devices
- Counter electrode in smart windows
- Transparent heat mirrors
- Anti-ferromagnetic layers [5]

## 1.6 References

1. M.T.Hutchings, E.J.Samuelsen, *Phys. Rev. B*, 6, (1972), 3447-3461.
2. I.Fasaki, A.Koutoulaki, M.Kompitsas, C.Charitidis, *Appl. Surf. Sci.*, 257, (2010), 429–433.
3. S.Sriram, A.Thayumanavan, *Int. J. Mater. Sci. Eng.*, 1, (2014), 118–121.
4. I.Hotovy, J.Liday, H.Sitter, P.Vogrincic, *J.Electr. Eng.*, 53, 11, (2002), 11–12.
5. M.F.Kuhaili, S.H.A.Ahmad, S.M.A.Durrani, M.M.Faiz, A.Ul-Hamid, *Materials Science in Semiconductor*, 39(2015), 84-89.

There are many other ways of preparing NiO thin films for example sol-gel, sputtering, chemical vaporization etc. Here is the literature survey of NiO thin films prepared by various techniques and oscillating compression measurement of Langmuir monolayer.

### 2.1 Deposition of NiO thin films by various other techniques

**Y.M Lu et al 2002 [1]:** NiO thin films were synthesised by RF Magnetron sputtering onto silicon and corning 7059 glass substrates. It was concluded that thin films resistivity crystalline size increases (12.1 nm to 30.2 nm) as substrate temperature increases (100°C-400°C).

**H.L.Chen et al 2005 [2]:** NiO thin films were deposited by RF Magnetron sputtering at different temperatures and RF powers on different substrates. It was concluded that resistivity (16.7Ωcm) increases with increase in sputtering power from 100 to 200W at constant temperature. Larger grain size (11.42nm-18.17nm) and more perfect crystalline structure was induced by higher substrate temperature which lead to low resistivity of NiO thin films.

**S.Y Han et al 2006[3]:** Chemical bath deposition technique was used for depositing NiO thin films of thickness 180 nm from an aqueous solution made of nickel sulphate, potassium persuphate, and ammonia at room temperature. The growth mechanism of NiO was studied which strongly depends upon mixing condition.

**S.A. Mahmoud et al 2011[4]:** Both crystalline and non-crystalline NiO thin films of 45 nm thickness and 3.9 μm<sup>2</sup> mean grain size area were synthesized by Spray Pyrolysis Technique(SPT) at different temperatures from 225 to 350°C using nickel acetate tetra hydrate solution onto glass substrates. Cubic single phase structure of NiO was confirmed from the results.

**M.Z.Sialvi et al 2013[5]:** Aerosol -Assisted Chemical Vaporization Deposition (AACVD) was used for preparing NiO thin films. Electrochromic properties of NiO and their

dependence on number of layers was studied. Thickness was changed from 536nm to 964nm by varying number of layers from 50 to 500.

**S.Sriram et al 2013[6]:** Nickel oxide thin films were prepared by low cost-simplified spray pyrolysis technique using aged and fresh precursor solution. Film deposited from the aged solution has more grain size (60.3nm) than the film deposited by fresh solution. Although film prepared from fresh solution (2.271 $\Omega$ cm) has low resistivity than aged precursor solution (2.725 $\Omega$ cm).

**I.Sta et al 2014[7]:** Undoped and Li doped NiO thin films were fabricated on glass substrate by sol-gel technique. Grain size (60nm-120nm) and thickness (150nm to 600nm) increases with increase in number of layers (1-5). As more number of layers were deposited thickness of films increases. It was determined that for obtaining high transparency four layers of undoped NiO were suitable. As lithium concentration increases resistivity of film decreases, so these films can be used as transparent conductors.

**M. Jlaesi et al 2014[8]:** Nickel oxide thin films were prepared by sol-gel combined with spin-coating technique onto glass substrate. From results it was concluded that 600°C is suitable temperature for preparing NiO thin films with p-type conductivity and high optical transparency. As number of layers increases from 1 to 5 grain size increases from 4nm to 19nm. Increase in thickness (14nm) of thin films result in decreased transmittance.

**M.F.A.Kuhaili et al 2015[9]:** NiO thin films were fabricated on silver (Ag) substrate by thermal evaporation technique. NiO thin films were tested for possible use in transparent heat mirrors. NiO thin films of thickness 30nm have large grain size (30.1nm), high visible transparency and high infrared reflection was characterized by AFM, XRD.

**M.A.R.Abdullah et al 2016[10]:** NiO thin films were synthesized at different annealing temperature by sol-gel method and quality of the surface was characterized using AFM. Surface roughness (0.915-1.578 nm) of thin films increases with annealing temperature (450°C).

## 2.2 Effect of pH on Langmuir monolayer

**J.B.Peng et al 2001[11]:** Ionization of stearic acid (carboxylic acid) in a floating monolayer was affected by pH of subphase. At high pH divalent cation tend to cause contraction of monolayer, Cd and Pb have more covalent character to their bonding with stearic acid as compared to other divalent ions.

**L.K.Brar et al 2005[12]:** Langmuir monolayer of NiA arachidate was prepared on Langmuir trough and characterized by surface pressure-area isotherms at different pH values. As pH varies from 4.8 to 7.4 incorporation of Ni (II) increases though mean molecular area decreases.

**R.Kaur et al 2014[13]:** Bent -core liquid crystals having alkyl chains at both ends were fabricated on silicon substrate by Langmuir Blodgett technique. Increasing pH of the subphase results in increased alkyl length due to van der Waals interaction. Low pH solutions was stable at high pressures.

## 2.3 Oscillating Barrier Measurement

**J.T.Petkov et al 2000[14]:** Langmuir technique is used for measuring surface shear elasticity modulus and dilatational modulus of gel like protein layer on air-water interface using oscillating barrier method. The stress response to deformation in Langmuir trough is measured by different orientations of wilhelmy plate: parallel and perpendicular to barriers. It was investigated that there is rise in elastic moduli with increasing protein content.

**D.Y.Zang et al 2010[15]:** Silica nanoparticle layers rheological behaviour at air-water interface was investigated. It was confirmed that elastic response to continuous step is same as oscillatory compression. Compressed layers (Langmuir monolayer) were more homogeneous and rigid whereas deposited layers were less rigid and more viscoelastic.

**R.Kaur et al 2013[16]:** Surface viscoelastic properties of ferroelectric liquid crystal monolayer was characterized by oscillation method as a function of surface pressure. It was concluded that in condensed phase elastic modulus and viscous modulus has higher values where as in liquid expanded phase has negative values of elastic modulus and viscous modulus.

**K.L.Harrison et al 2015[17]:** Monolayers of graphene oxide was formed on Langmuir trough. Oscillating barrier measurements were taken for characterizing resulting compressive and shear moduli as a function of surface pressure. It was proposed that angle dipping is only beneficial for that monolayers which exhibit a shear modulus.

## **2.4 Deposition of thin films by Langmuir Blodgett techniques**

**H.Sakai et al 2001[18]:** Langmuir monolayers of zinc stearate and zinc-12-hydroxy-stearate on water surface were formed. When zinc stearate was compressed the structure around carboxylic group changes however orientation and conformation hydrocarbon chain did not change. Hence concluded that stearate monolayers were different from zinc-12-hydroxy-stearate monolayers.

**N.Kumar et al 2013[19]:** The effect of  $\text{Ca}^{2+}$  and  $\text{Na}^+$  ions were compared by changing their concentrations in both subphase before the LB transfer and in the droplets up to dried layers were replaced. By varying composition of the droplets stability effect of  $\text{Ca}^{2+}$  was confirmed.

## **2.5 Oxide thin films by Langmuir Blodgett techniques**

**N.Matsuura et al 1997[20]:** CdO thin films were synthesised on Si/SiO<sub>2</sub> substrate by LB technique. The oxide films was continuous with  $10^4$ - $10^5$   $\Omega\text{m}$  resistivity formed at 220-300°C. Cd arachidate 50 layers were deposited on silicon substrate with 20-150nm thickness.

**S.Sharma et al 2015[21]:** NiO layers were fabricated on Si/SiO<sub>2</sub> substrate by Langmuir Blodgett technique. Structural and electrical properties of NiO thin films of thickness 5nm were investigated by X-ray Photoelectric spectroscopy, EDS (Energy Dispersive X-ray Spectroscopy) and AFM (Atomic Force Microscopy). The results of characterization shows that combination of NiO/SiO<sub>2</sub> worked as diffusion barrier up to 772K.

**I.Azad et al 2016[22]:** In this paper zinc stearate thin films were deposited on Au/Cr coated quartz and silicon substrate. 20 layers of ZnO were fabricated at 550°C annealing temperature having 100nm thickness (grain size was 5nm).

## 2.6 References:

1. Y.M.Lu, W.S. Hwang, J.S. Yang, H.C.Chuang, *Thin Solid Films*, 420-421(2002), 54-61.
2. H.L.Chen, Y.M.Lu, W.S.Hwang, *Surface and Coating Technology*, 198(2005), 138-142.
3. S.Y.Han, D.H.Lee, Y.J.Chang, S.O.Ryu, T.J.Lee, C.H.Chang, *Journal of Electrochemical Society*, 0013-4651(2006),153.
4. S.A.Mahmoud, S.Alshomer, M. A.Tarawnh, *Journal of Modern Physics*, 2(2011) 1178-1186.
5. M.Z.Sialvi, R.J.Mortimer, G.D.Wilcox, A.M.Teridi, T.S.Varley, K.G.Wijayantha, C.A.Kirk, *Appl. Mater. Interfaces*, 5(2013), 5675-5682.
6. S.Sriram, A.Thayumanavan, *International Journal of Materials Science and Engineering*, 1 (2013), 118-121.
7. I.Sta, M.Jlassi, M.Hajji, H.Ezzaouia, *Thin Solid Films*, 555(2014), 131-137.
8. M.Jlassi, I.Sta, M.Hajji, H.Ezzaouia, *Materials Science in Semiconductor Processing*, 21(2014), 7-13.
9. M.F.Kuhaili, S.H.A.Ahmad, S.M.A.Durrani, M.M.Faiz, A.U.Hamid, *Materials Science in Semiconductor Processing*, 39(2015), 84-89.
10. M.A.R.Abdullah, M.H.Mamat, A.S.Ismail, M.F.Malek, S. A.H.Alrokayan, *AIP Conference Proceedings*, 020013(2016), 1733.
11. J.B.Peng, G.T.Barnes, I.R.Gentle, *Advances in colloidal and interface science*, 91(2001), 163-219.
12. L.K.Brar, P.Rajdev, A.K.Raychandhari, D.Chatterji, *Langmuir*, 21(2005), 10671-10675.
13. R.Kaur, G.K.Bhullar, N.V.S. Rao, K.K. Raina, *Liquid Crystals*, 8-17(2014), 1366-5855.
14. J.T. Petkov, T.D. Gurkov, *Langmuir*, 16(2000), 3703-3711.
15. D.Y.Zang, E.Rio, D.Langevin, B.Wei, B.P.Binks, *European Physics Journal*, 31(2010), 125-134.
16. R.Kaur, G.K.Bhullar, K. K. Raina, *AIP Conference Proceedings*, 1377(2013), 1536.

17. K.L. Harrison, L.B. Biedermann, K.R. Zavadil, *Langmuir*, 31(2015), 9825-9832.
18. H.Sakai, J.Umemura, *Colloid and Polymer surfaces*, 280(2002), 316–321.
19. N.Kumar, L.Wang, I.Siretanu, M.Duits, F.Mugele, *Langmuir*, 29(2013), 5150–5159
20. N.Matsuura, D.J.Johnson, D.T.Anm, *Thin films*, 295(1997), 260-265.
21. S.Sharma, M.Kumar, S.Rani, D.Kumar, C.C. Tripathi, *The Minerals, Metals & Materials Society and ASM International 2015*, 46A(2015), 3166.
22. I.Azad, M.K.Ram, D.Y.Goswami, E.Stefanakos, *Langmuir*, 32(2016), 8307-8314.

### 3.1 Introduction

**Langmuir monolayer** is monolayer formed at gas-liquid or liquid-liquid interface. When these monolayers are deposited on solid substrates then these are called **Langmuir-Blodgett films**. Substrates can be hydrophobic (“water repelling”) or hydrophilic (“water loving”). Some examples of these substrates are glass, silicon, graphite, silver, gold, mica etc. [1].

In this method the monomolecular or multimolecular films of an amphiphilic (hydrophobic head and hydrophilic tail) substance are formed on the water surface and then transfer on solid substrate.

#### **Why LB films are involved in present work?**

Why we preferred LB technique? LB technique is very good for preparation of thin films because of

- a) Sharp control of monolayer thickness.
- b) Homogeneous deposition of monolayer over large areas [2].
- c) Deposition of multilayers with varying layer composition.
- d) Control over internal layer structure.
- e) Preparation multilayers by changing the nature, deposition pressure and other parameters of the thin films.
- f) Deposition is possible on any kind of substrate.

### 3.2 Formation of Langmuir Monolayer

Monolayer is layer of closely packed single atoms, molecules or cells. Langmuir monolayer is insoluble monolayer made by spreading insoluble organic material on liquid subphase. Monolayer is composed of amphiphilic compounds.

Monolayer is formed by spreading a solution of surfactant (e.g. stearic acid in suitable solvent (chloroform) drop-wise on the surface of subphase) with the help of microsyringe. The solvent chosen should be insoluble in subphase which should evaporate after 15-20 minutes. Surfactant spreads uniformly as monolayer on subphase. With the help of moving barriers monolayer is compressed and is known as Langmuir film. When these films are transferred on solid substrate then these films are known as Langmuir Blodgett films.

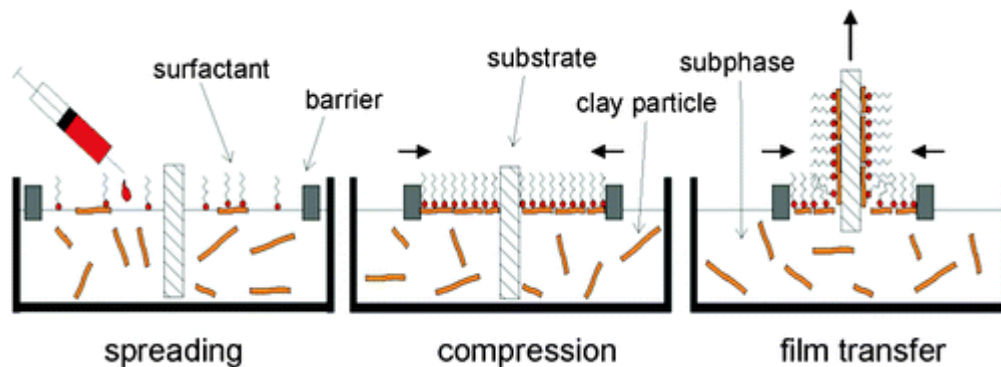


**Figure3.1:** Schematic Diagram of Formation of Langmuir Blodgett films. [3]

### 3.3 Pressure-Area Isotherm

Pressure-Area isotherm reveals many properties of monolayer. As it is carried out at constant temperature, so known as pressure-area isotherm or simply isotherm.

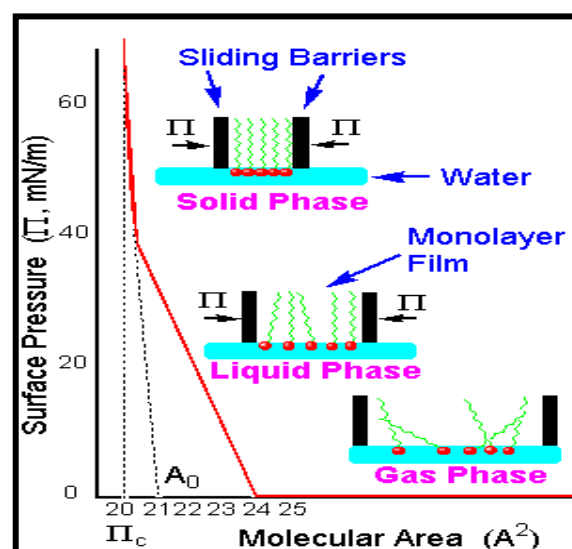


**Figure3.2:** Schematic diagram of pressure-area isotherm [1].

Initially, when molecules are spread on subphase (water) they are loosely packed which indicates gas phase as shown in figure when barriers are at rest which possess high molecular area and low surface pressure. As barriers are closed, compressibility changes due to rapid change in surface pressure with molecular area and we have liquid phase. When barriers are further closed high surface pressure and low molecular area is obtained to get incompressible solid phase.

The surface pressure is measured by whilmy plate. It is given by:

$$\Pi = \gamma_0 - \gamma \quad (3.1)$$

Where  $\gamma$  is surface tension (attraction between liquid molecules) of the monolayer-covered subphase and  $\gamma_0$  is the surface tension of the pure liquid subphase. It reveals many interfacial, interaction properties [4, 5].

### 3.4 Deposition Methods

To form Langmuir Blodgett film we have to transfer or deposit monolayers on solid substrate. There are two methods for transferring monolayers on solid substrate these are:

1. Horizontal deposition(Langmuir-Schaefer technique)
2. M5Vertical deposition(Langmuir-Blodgett technique )

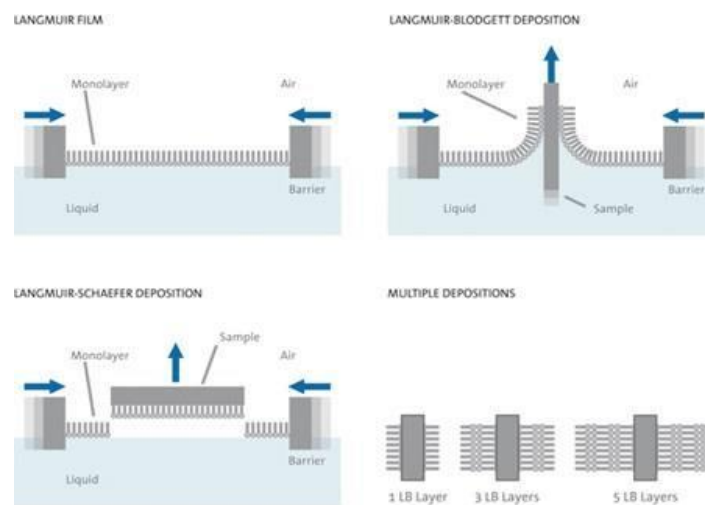


**Figure3.3:** Schematic diagram showing horizontal and vertical deposition [2].

**Horizontal Deposition:** Horizontal deposition is also known as Langmuir-Schaefer technique as it was introduced by Langmuir and Schaefer. In this Langmuir layer is horizontally transferred from an air-water interface to hydrophobic solid substrate.

**Vertical deposition:** It was first introduced by Langmuir and Blodgett, so known as Langmuir-Blodgett technique. In Langmuir-Blodgett technique Langmuir layer is vertically transferred on solid substrate (may be hydrophobic or hydrophilic) from an air-water interface.

### 3.5 Types of Langmuir Blodgett deposition

There are 3 types of Langmuir Blodgett deposition named as:

- a) X-Type deposition
- b) Y-Type deposition
- c) Z-Type deposition

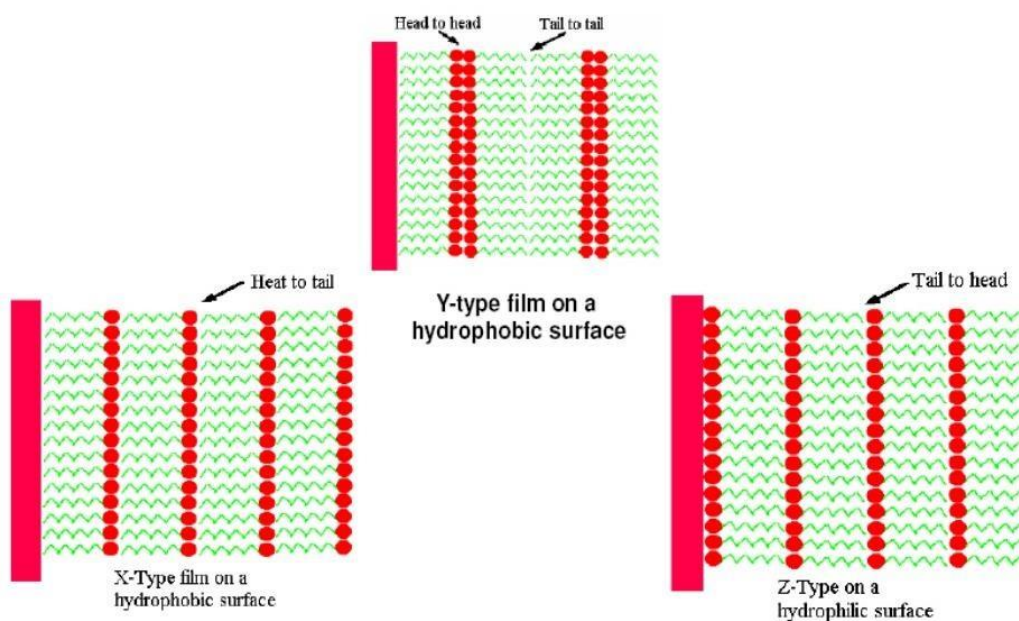


**Figure 3.4** Schematic diagram showing X, Y, Z deposition types of Langmuir Blodgett technique [1].

**X-Type deposition:** When deposition takes place only by down stroke on hydrophobic substrate then such deposition is called X-type deposition. Mostly X-Type deposition is used for high pH values.

**Y-Type deposition:** When layers are transferred by up and down stroke then such deposition is called Y-type deposition. This type of deposition is mostly preferred for fatty acids.

**Z-Type deposition:** When deposition takes place only by up stroke on hydrophilic substrate then such deposition is called Z-type deposition. Z- type deposition is seen in aromatic molecules that have no hydrocarbon chains.

For obtaining stable condensed film surface pressure ( $20\text{-}40\text{mNm}^{-1}$ ) and temperature ( $15\text{-}20^\circ\text{C}$ ) are maintained. Parameters that effect type of LB film are nature and type of solid substrate, nature of spread film, subphase composition, deposition speed.

The quality and quantity of transferred monolayer can be measured by Transfer Ratio (TR).

$$TR = \frac{\text{decrease in monolayer area } (A_L)}{\text{area of the substrate } (A_s)}$$

So, TR is ratio of decrease in monolayer during the deposition stroke to the area of the substrate. TR is always equal to 1 for ideal transfer [1].

### 3.6 Oscillating Barrier Measurement

Mechanical properties like elasticity, strain, stress etc. are measured by oscillating barrier method. Surface viscoelastic properties of nickel stearate monolayer can be determined by oscillating barrier method. In oscillating barrier method barriers start oscillating after achieving target value under given frequencies as shown in figure.

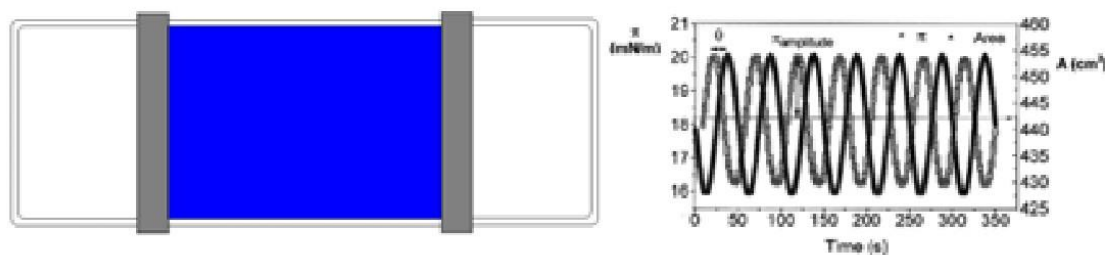


**Figure3.5:** Oscillating barrier and sinusoidal waves formed by compression and expansion [2].

$$A = A_0 - A_m \sin(\omega t) \quad (3.2)$$

$$\Pi = \Pi_0 - \Pi_m \sin(\omega t + \theta) \quad (3.3)$$

Where  $A_0$  and  $\Pi_0$  are average area and pressure respectively.

$A_m$  -change in amplitude.

$\Pi_m$  -change in surface pressure.

t -time

$\omega$  -angular frequency

$\theta$ - loss angle(phase change between response and deformation)

We can calculate G (Elastic modulus),  $G'$  (Storage modulus),  $G''$  (viscus modulus).

$$G = \frac{\text{dilatational stress}}{\text{dilatational strain}} = \Pi_m \times \frac{A}{A_m} \quad (3.4)$$

$$G = G' + iG'' \quad (3.5)$$

Where G is complex quantity and  $G'$  (elasticity component) is real part and  $G''$  (viscous component) is imaginary part.

$$G' = G \cos \theta \quad (3.6)$$

$$G'' = G \sin \theta \quad (3.7)$$

$$\text{loss angle} = \frac{G''}{G'} \quad (3.8)$$

As monolayer becomes condense its viscous modulus increases and elastic modulus goes on decreasing. [6]

### 3.7 Langmuir-Blodgett Technique's Experimental Setup

**Various parts of LB setup are:**

**Trough:** It is Teflon surface on which monolayer is formed and further compressed or expanded on surface therefore modifying area per molecule .There is deposition well for deposition of layers.

**Barriers:** Barriers slides parallel to the walls of trough. Barriers are also made of Teflon that is hydrophilic material which ensure that film does not escape these barriers.

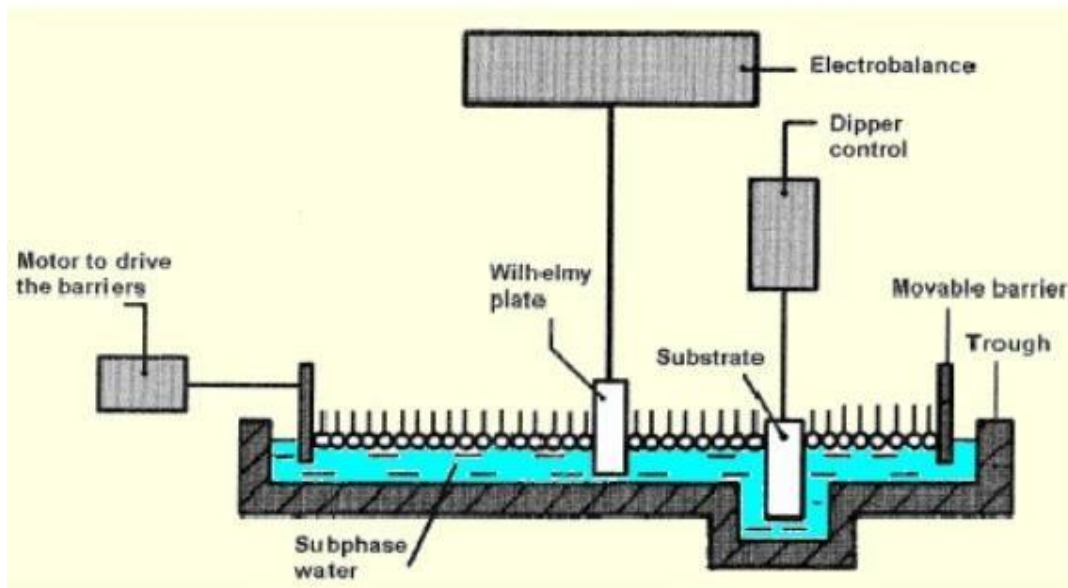


**Figure 3.6:** Systematic diagram showing Langmuir Blodgett Technique [2]

**Balance:** A platinum plate of dimensions 38mm ×19.62mm ×10mm used for measuring surface pressure is named as Wilhelmy plate. The force acting on this plate is measured by electro balance so called surface balance.

**Dipper:** For depositing layers on substrate it is held in dipper clip. Further speed and all other essential parameters are controlled for precise deposition.

**Layer Builder:** Layer builder is an interface unit. It is connecting unit between computer and connected devices of LB apparatus. It displays surface pressure and barrier position on it [2].

### 3.8 Advantages

In LB technique we can control the thickness with precision of monolayer. We can deposit layers on any type of substrate and further characterize elasticity, surface potential and visco-elastic properties. Ultra-thin films can be formed by this technique. There is homogeneous deposition over the substrate surface.

### 3.9 Disadvantages

This technique is time consuming especially if thick films are required. Temperature plays a vital role in the formation of thin film, slight variation results in monolayer property change. Small contamination can destroy the formation of the film. These films have poor mechanical and chemical stability on the surface of the trough.

### 3.10 References:

1. M.C. Petty, Handbook of Langmuir-Blodgett Films, Cambridge University Press, (1996).
2. KSV Instruments Software Manual LB device.
3. R.H.A.Ras, Y.Umemura, C.T.Johnston, A.Yamagishi, *Phys. Chem*, 9(2007), 918.
4. G.Roberts, Ed.Langmuir Blodgett Films, Plenum Press: New York, (1990)
5. B.P.Binks, *Adv. Colloid Interface Sci.*, 34 (1991), 343.
6. R.Kaur, G. K. Bhullar, K. K. Raina, *AIP Conference Proceedings*, 1377(2013), 1536.

This chapter deals with materials and methods used for performing experiments. Characterization techniques used for thin films are also explained.

#### **4.1 MATERIALS USED**

Most important chemicals and reagents used for preparation of Langmuir Blodgett Thin Films are:-

1. Nickel (II) Sulfate ( $\text{NiO}_4\text{S}$ , Sigma Aldrich, Anhydrous with 99.99%, M.W. 154.76g/mol).
2. Sodium Hydroxide Pellets ( $\text{NaOH}$ , Loba Chemie Pvt. Ltd, 98%, M.W. 40g/mol).
3. Methanol ( $\text{CH}_4\text{O}$ .SDFCL, 98.3%, M.W.32.04g/mol).
4. Propan-2-ol ( $(\text{CH}_3)_2\text{CHOH}$ , Fisher Scientific, 99.7%, M.W.60.10g/mol).
5. Chloroform ( $\text{CHCl}_3$ , SDFCL, 99%, M.W.119.38g/mol).
6. Sulphuric acid ( $\text{H}_2\text{SO}_4$ , SDFCL, 98%, M.W. 98.07g/mol).
7. Hydrogen Peroxide ( $\text{H}_2\text{O}_2$ , Loba Chemie Pvt. Ltd, M.W. 34.01g/mol).
8. Stearic acid ( $\text{C}_{17}\text{H}_{35}\text{COOH}$ , Sigma Aldrich, > 98.5%, M.W.284.48g/mol).
9. Acetone ( $\text{C}_3\text{H}_6\text{O}$ , SDFCL, 99%, M.W.58.08g/mol).
10. Deionized water (DI) used was acquired from Millipore Q3 system with resistivity of  $18.2 \text{ M}\Omega^{-1}$ .
11. Borosil microscope slides with plain ground edges of dimensions 76 mm×26 mm×1.25 mm (Refractive Index (Ne)  $1.53 \pm 0.02$ ) cut in 15 mm×26 mm× 1.25 mm dimensions were used as substrates.

#### **4.2 Methods**

#### **4.2.1 Cleaning of Trough:**

Before putting solution on trough cleaning of trough is must. Nitrile gloves were used to avoid contamination. Teflon trough was first cleaned by methanol with soft brush and then by propan-2-ol. Final rinsing of the trough was with deionized water.

#### **4.2.2. Cleaning of Substrates:**

Borosil slides were cleaned by piranha cleaning method sonicated in DI water for five minutes. This was followed by sonication in acetone, ethanol and deionized water for five minutes each respectively.

#### **4.2.3. Preparation of Subphase:**

Langmuir monolayers were formed on the 0.1mM Nickel sulphate solution. The pH of solution was modified by NaOH solution of 0.1mM molarity.

#### **4.2.4. Preparation of Langmuir and Langmuir Blodgett films:**

KSV NIMA apparatus having minitrough of 24300mm<sup>2</sup> surface area was used for forming Langmuir monolayer and Langmuir Blodgett films. Trough and barriers both were made of Teflon. 30µl stearic acid solution formed with chloroform of 0.75mg/ml concentration was spread on aqueous subphase using Hamilton Micro Syringe. Solvent takes 15 to 20 minutes for evaporation after that compression process was started. Isotherms measurement was carried out at 15mm/min.

For deposition of LB films target was set at 30mN/m, dipping speed was 7mm/min. Films were allowed to stabilize before dipping and dried for 2 minutes for drying above the liquid surface. Complete transfer of monolayer was only considered if transfer ratio should be nearly 1.0.

#### **4.2.5. Oscillating Barrier Method:**

For oscillating barrier measurement gain control was 1.5, change in area was  $0.8A_0$  and rate was 15mm/min. Frequency was varied from 30 mHz to 50mHz in steps of 5 Hz in each experiment.

#### 4.2.6. Drying and Calcination protocol:

##### Drying

- a) After depositing LB thin films the sample was dried under vacuum for 45 minutes.
- b) Further they was heated at 120°C for removal of any absorbed water.

##### Calcination protocol

- a) Heat at 380°C for one hour for decomposing stearic acid.
- b) Further heating at 600°C for six hours for formation of NiO films.

This heating protocol was based on literature survey of earlier work in the group [1-3].

Samples detail:

SAMPLE	pH	No. of layers
69Ni15	6.9	15
83Ni15	8.3	15
79Ni10	7.9	10
79Ni15	7.9	15
79Ni19	7.9	19

### 4.3. Characterization Techniques:

#### 4.3.1. Surface Pressure ( $\pi$ ) - Area (A) Isotherm:

The basic monolayer properties of thin films in Langmuir Blodgett Technique were studied by pressure-area isotherms. Already discussed in detail in 3.3.

$$\text{Elasticity} = -A \times \left( \frac{d\Pi}{dA} \right)_{T,n} \quad (4.1)$$

Where A is area and n is number of moles. Hence elasticity is simply found from pressure-area isotherms.

### 4.3.2. Field Emission Scanning Electron Microscopy (FE-SEM):

SEM is a type of electron microscope in which images of a sample are produced by focusing a narrower electron beam to a spot of nearly 20-100 nm diameter as shown in figure 4.1 and made to scan the sample surface in a raster.

Different imaging modes of SEM and their resolutions are given below in the table.

<b>Modes</b>	<b>Resolution</b>
Secondary electrons	3 nm
Back scattered electrons	100 nm
Characteristic x-rays	1-2 $\mu\text{m}$
Cathodo-luminescence	2 $\mu\text{m}$
Current	500 nm
Field emission	20 nm

The most common SEM mode is detection of secondary electrons emitted by atoms excited by the electron beam. Samples are first coated with an extremely thin layer (1.5 - 3.0 nm) of gold or gold palladium so that samples must be able to sustain the high vacuum. Sample grain size, surface roughness, porosity, samples homogeneity and particle size distributions are evaluated using SEM [4].

In FE-SEM electrons are generated by field emission source. FESEM provides topographical information at very high magnifications (10x to 300,000x). It works on principle that field emission source in the electron gun of a SEM produces a narrow beam at low as well as high electron energy which increase its resolution. Systematic diagram of FE-SEM is shown in figure 4.1.

We have used HITACHI SU8010 and Carl Zeiss Merlin Compact Field Emission Scanning Electron Microscope for FESEM studies.

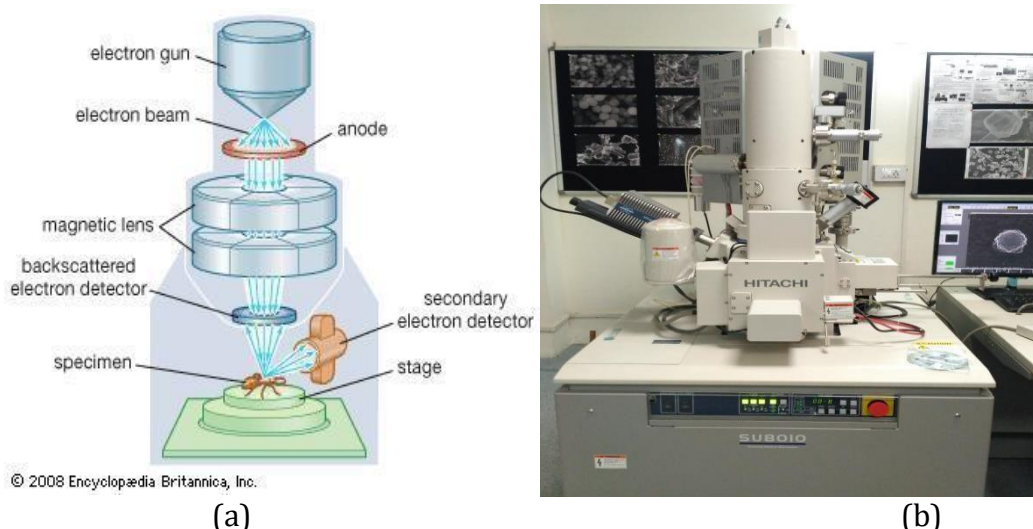


**Figure 4.1:** (a) Systematic diagram of FE-SEM [4] (b) Laboratory view of FE-SEM.

### 4.3.3. Ultraviolet–Visible spectroscopy (UV-Vis):

In UV-Visible (Ultraviolet–Visible) spectroscopy ultraviolet means that the information will come from a specific region of the electromagnetic spectrum called the ultraviolet region (190 to 400 nm U.V. Region and 400 to 800 nm Visible Region). UV-Vis spectroscopy is the measurement of the transmittance of a beam of light after it passes through a sample. So from this transmittance absorbance can be determined. UV is preferred for detection of functional groups, detection of impurities, qualitative analysis and quantitative analysis.

We have used Shimadzu (Japan) UV-2450 Ultraviolet visible spectroscopy for UV-Vis studies.

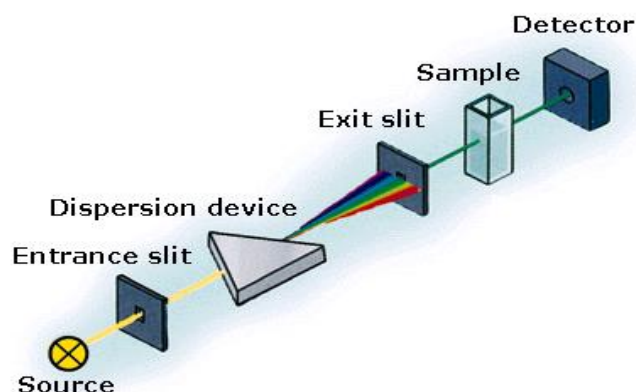


**Figure 4.2:** Systematic diagram of Ultraviolet–visible spectroscopy (UV-Vis) [4].

#### 4.3.4 XRD

XRD is a rapid analytical technique used for studying the phase and structure of crystalline material. XRD measures the shape, size, internal stress of small crystalline regions and average spacing between layers and rows. Systematic diagram of XRD is shown in figure 4.3. Bragg's equation is used for calculating interplanar spacing values.

$$n\lambda = 2d \sin \theta \quad (4.2)$$

where  $n$  is order of reflection,  $\lambda$  is the wavelength of source and  $\theta$  is Bragg's angle of diffraction.

For the XRD studies we have used Philips XPERT- PRO MPD X-Ray Spectrometer.

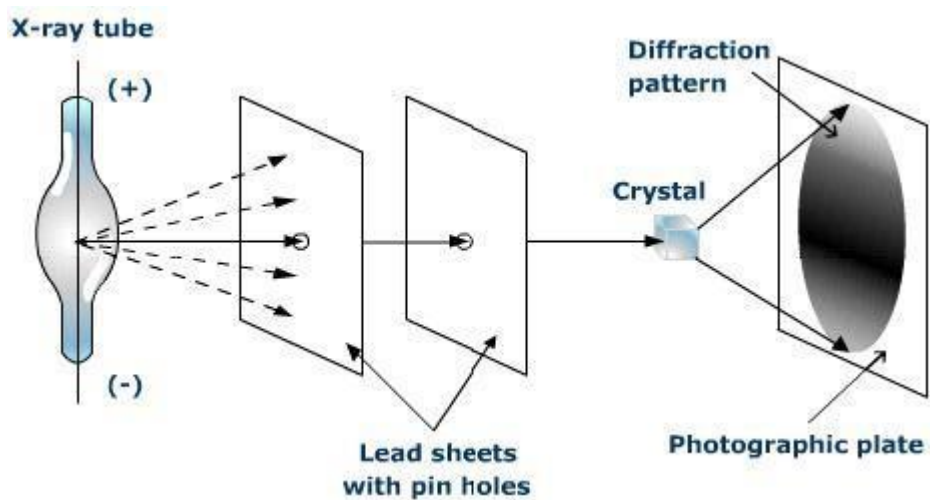


**Figure 4.3:** Systematic diagram of XRD.

#### 4.4 References:

1. Palvi, P.Sharma(Guide), L.K.Brar(Guide), *Masters Theses@SPMS, TuDR*, (2016).
2. S.Sharma, M.Kuma r, S.Rani, D.K umar, C.C. Trip at hi, *The Minerals, Metals & Material s Society an d ASM International 2015* , 46A( 2015), 3166.
3. M.Jlassi, I.Sta, M.Hajji, H.Ezza ouia, *Materials Science in Semicondu ctor Processing* , 21(2014), 7–13.
4. P.R Khan gaon ka r, *An Int roducti on to Materi als Cha ract eri zati on*, Penram International Publishing, (2010).

**Overview**

This chapter includes results obtained from various characterization techniques such as Surface Pressure-Area Isotherms, oscillating-barrier characterization, XRD, FE-SEM, EDS, UV-Visible spectroscopy that we obtained for the Langmuir, Langmuir Blodgett films of nickel stearate and the final oxide films.

**5.1. Surface Pressure ( $\pi$ ) -Area (A) Isotherms:**

$\pi$ -A isotherms have been used to characterize the monolayers formed on the air-subphase interface. All the data is taken at the subphase temperature of 20 °C and barrier speed of 15 mm/min. The elasticity for the monolayer can be determined from the isotherm by:

$$\mathbf{E} = - \frac{d\pi}{\left(\frac{dA}{A}\right)} \quad (5.1)$$

This elasticity is termed as static elasticity as it is determined from the instantaneous deformation of monolayer and does not include any dissipative effects.

**5.1.1 Effect of subphase concentration:**

To determine the effect of subphase concentration on the quality of Langmuir monolayer being deposited the  $\pi$ -A isotherms of stearic acid (SA) spread on different concentration NiSO<sub>4</sub> solution subphases were analysed. To insure incorporation of Ni<sup>2+</sup> in the monolayer the pH is made basic (7.3). Figure 5.1 shows the isotherms obtained for different concentrations of NiSO<sub>4</sub>. Compaction of monolayer is signature of divalent ion incorporation. Table 5.1 gives the mean molecular area (Mma) for liquid and solid phases as well as the static elasticity of the solid phase calculated from the isotherms. The data shows that as the NiSO<sub>4</sub> concentration increases in the mean molecular area of the liquid as well as solid phase decreases and static elasticity of the solid phase increases. These changes clearly indicate compaction as well as an increase in the intermolecular interactions as a result of increasing incorporation of Ni<sup>2+</sup> in the monolayers.

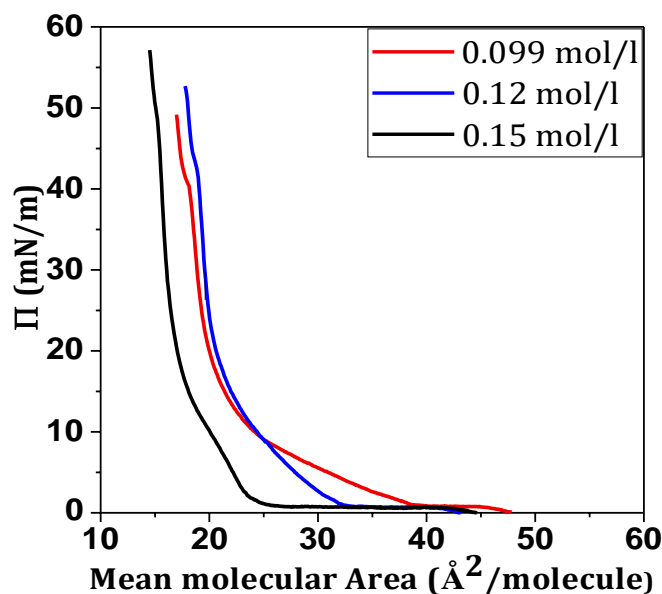


**Figure 5.1:** Surface Pressure-Area Isotherms of Ni-stearate for different subphase concentrations.

**Table 5.1** Elasticity and mean molecular area for liquid and solid phases at different subphase concentration.

Concentration (mol/l)	Static Elasticity (mN/m)	Mma of Liquid phase (Å <sup>2</sup> /molecule)	Mma of Solid phase (Å <sup>2</sup> /molecule)
0.099	292.93	38.52	22.86
0.12	389.18	32.22	21.64
0.15	395.68	24.90	20.44

To ensure adequate Ni<sup>2+</sup> incorporation in the monolayers all the further data is taken for the subphase concentration of 0.15 mol/l.

### 5.1.2 Effect of pH

Figure 5.2 presents isotherms of stearic acid on DI water and NiSO<sub>4</sub> solution as sub-phase for varying pH values. All Isotherms clearly show gas, liquid and solid phases as discussed earlier in chapter 3. The mean molecular area for liquid and solid phases as well as the static elasticity of the solid phase has been calculated from the isotherms and is given in table 5.2. The values obtained for stearic acid match those available in literature [1-3].

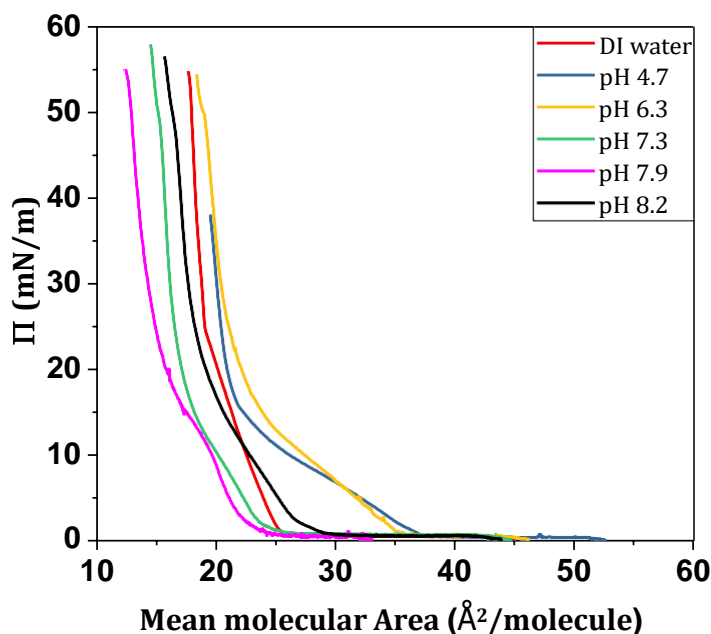


**Figure 5.2:** Surface Pressure-Area Isotherms of stearic acid on DI water and NiSO<sub>4</sub> for different sub-phase pH values.

**Table 5.2:** Static elasticity and mean molecular area (Mma) of liquid and solid phases for different subphase pH values.

Subphase	pH	Static Elasticity (mN/m)	Mma of Liquid phase (Å <sup>2</sup> /molecule)	Mma of Solid phase (Å <sup>2</sup> /molecule)
DI water	-	500.33	25.93	20.62
NiSO <sub>4</sub>	4.7	300.52058	37.68	22.34
NiSO <sub>4</sub>	6.3	326.17831	35.43	25.60
NiSO <sub>4</sub>	7.3	395.299	24.90	20.44
NiSO <sub>4</sub>	7.9	252.6971	24.178	18.54
NiSO <sub>4</sub>	8.2	328.6851	28.95	20.23

A comparison of the monolayers on DI water and low pH NiSO<sub>4</sub> (pH 4.7) subphase shows that the Mma increases and the static elasticity of the solid phase decreases for the latter. This clearly signal that at low pH Ni<sup>2+</sup> ions incorporated in the monolayer to form Ni-stearate is sufficient to disrupt the structure of the stearic acid monolayer but do not result in compaction. For the monolayers formed on the NiSO<sub>4</sub> subphase the Mma decreases with increasing pH (4.7 to 7.9) indicating higher compaction as a result of more Ni<sup>2+</sup> incorporation. For these monolayers the static elasticity value of the solid phase also

increases indicating an increase in the order and inter molecular interactions. A closer look at the data shows that even though the Mma decreases for the pH 7.9 sample the static elasticity actually decreases. This implies that increasing incorporation of  $\text{Ni}^{2+}$  ions in the monolayer with pH is resulting in compaction but also gives rise to a repulsive interaction among the ions. This is conjecture is substantiated when we increase the pH to 8.3 where the repulsive interactions are sufficient to counter even the compaction. This results in increased Mma and a smaller static elastic modulus.

Hysteresis isotherms refer to repeated compression and expansion cycles and gives information about the configuration retention of the system. A representative hysteresis curves for pH 7.3 is shown in figure 5.3. The complete reversibility of data clearly indicates that the mixed monolayer of Ni-stearate and Stearic acid are stable [4].

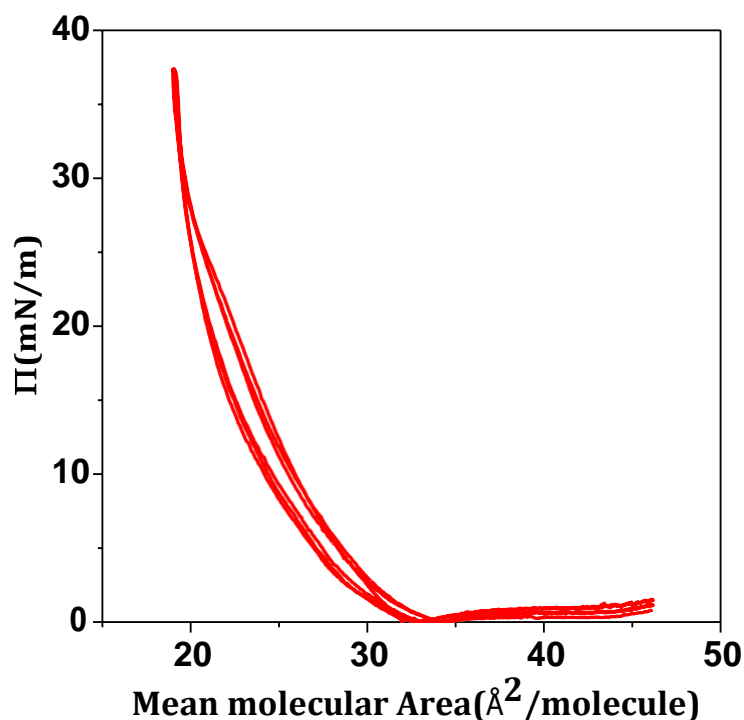


**Figure 5.3:** Surface pressure area hysteresis isotherm of nickel stearate at pH 7.3.

Based on these results it was decided to deposit the Langmuir-Blodgett monolayers of Ni-stearate at pH 7.9 since for this pH we get the maximum compaction as well as the maximum incorporation of Nickel.

## 5.2 Oscillating Barrier characterizations of Ni-stearate monolayers:

Oscillating barrier measurements are used to determine the dynamic elasticity of the monolayers. Dynamic elasticity measurements give information about the interaction forces as well as the relaxation processes within the films. Oscillatory barrier measurements to study the dynamic elasticity of the Ni-Stearate monolayers layers were performed in the solid phase at the surface pressure of 30 mN/m. The isotherms were formed for the barrier speed of 15mm/min. The inbuilt measurement software of the LB trough system is used to determine the dynamic viscoelastic properties namely,  $G$  (Elastic modulus),  $G'$  (Storage modulus),  $G''$  (viscous modulus) for each frequency.

### 5.2.1 Effect of barrier oscillation frequency:

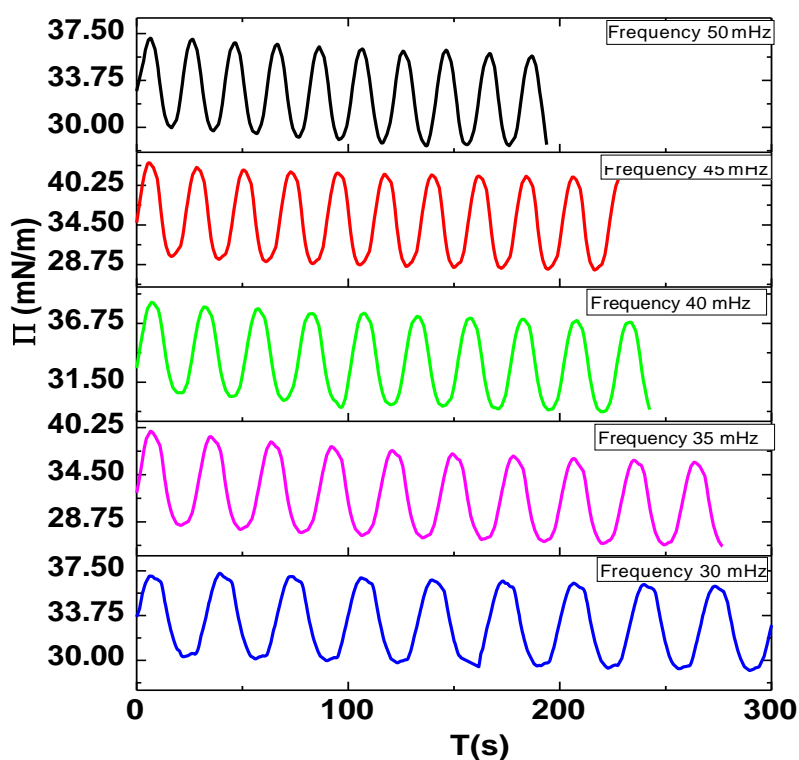


**Figure 5.4:** Surface pressure variations for barrier oscillation at different frequencies.

The dynamic elasticity involves the relaxation processes so the time scales over which the measurements are taken become important. For the present case the oscillation of barrier was done at different frequencies varying from 30 mHz to 50 mHz in steps of 5 mHz. The limits on the frequency are based on the fact that the wave generated cannot

be slower than the speed of the barriers and if it is too fast the relaxation processes will not become apparent. The set of frequencies were chosen based on the literature survey for similar systems [5]. The pH of 7.3 was chosen for these measurements as the monolayers show highest static elasticity for this pH. The figure 5.4 shows the surface pressure variations during the measurements. Table 5.3 and figure 5.4 give the dynamic viscoelastic properties data obtained from the analysis of these curves.

**Table 5.3:** Dynamic viscoelastic properties obtained from the analysis of curves obtained at different frequencies.

Frequency	G	G'	G''
30	171.06	151.54	79.36
35	297.54	281.91	95.16
40	386.65	364.49	129.01
45	344.23	282.91	196.13
50	363.04	341.63	122.82

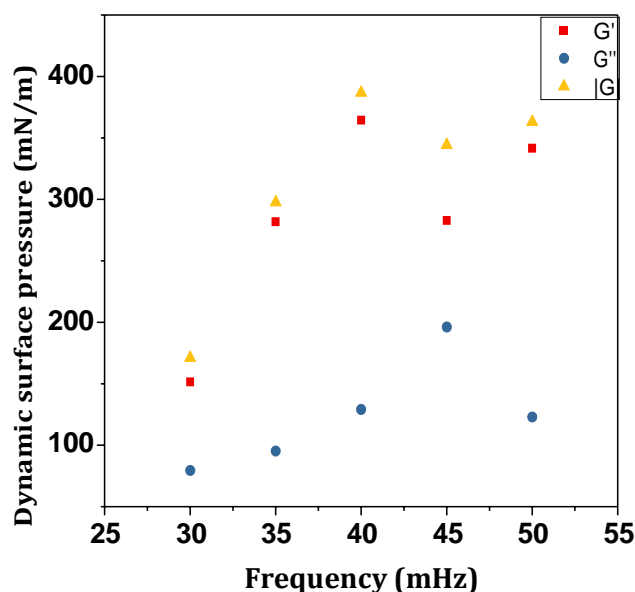


**Figure 5.5:** Variation in dynamic viscoelastic properties at different frequencies.

The dynamic elastic modulus of the monolayer increases with increasing frequency with maxima at 40 mHz. Further increase in oscillation frequency results in a decrease in the

value of the storage modulus which decreases the overall elastic modulus in spite of an increase in  $G''$ . This indicates that at this frequency (45 mHz) there is a relaxation process occurring in the film which may be interfering with intermolecular interactions/structure.

For determining the effect of pH on the dynamic elasticity we oscillate the barriers at 40 mHz frequency due to the stability of the system at this frequency.

### 5.2.2 Effect of subphase pH:

$\Pi$ -A isotherms clearly indicate that subphase pH plays an important role in determining the elastic properties of the Ni-stearate monolayers. To understand the effect of pH on the elastic and viscoelastic properties of the monolayers the oscillating barrier experiments at 40 mHz were performed for different subphase pH: 5, 6.5, 7.3, 8.3. Figure 5.6 shows the surface pressure oscillations for different pH values at 40 mHz frequency. Table 5.5 and figure 5.7 give the change in dynamic viscoelastic properties obtained from the analysis of these curves.

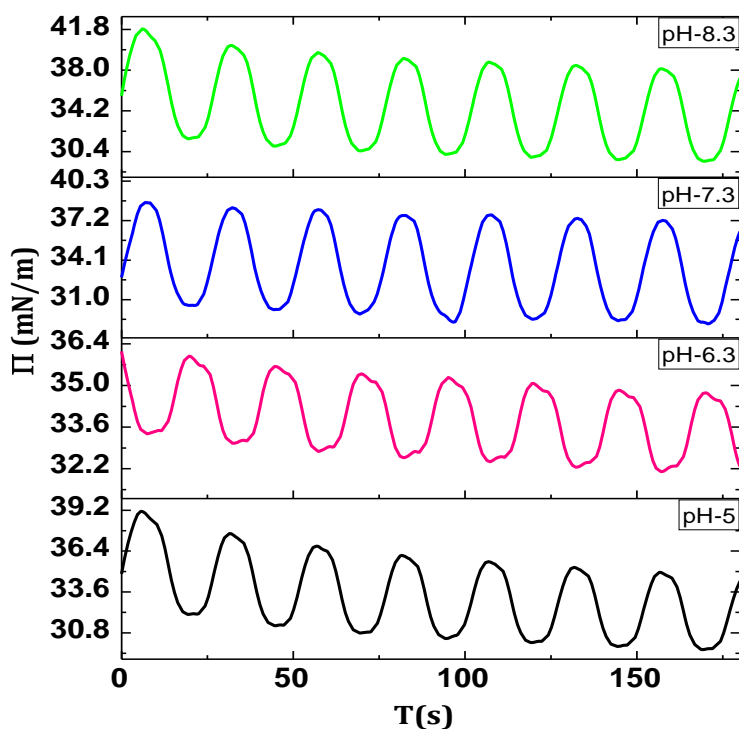


**Figure 5.6:** Surface pressure variations for barrier oscillation experiments for different subphase pH.

**Table 5.4:** Dynamic viscoelastic properties obtained from the analysis of curves obtained at different subphase pH.

pH	G	G'	G''
5	67.98	64.58	21.24
6.5	234.53	207.63	109.06
7.3	386.65	364.49	129.01
8.3	1369.08	171.93	1358.24

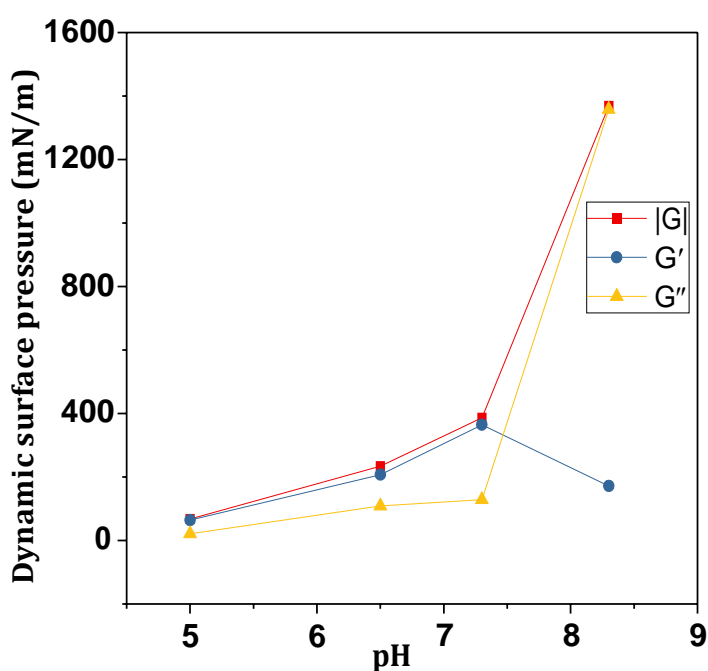


**Figure 5.7:** Variation in dynamic viscoelastic properties for different subphase pH values.

The data clearly shows that with increasing pH incorporation of Ni<sup>2+</sup> ions increases the interactions within the layer resulting in an increase in G'. At the same time the G'' also increases but not very sharply. A very sudden change is observed for pH 8.3 where the dynamic elastic modulus increases sharply. But a close look at the data shows that this increase in |G| is due to increase in viscous modulus whereas the elastic modulus actually decreases. This supports our earlier conjecture that at very high pH the repulsive interactions between the Ni<sup>2+</sup> ions leads to reduced intermolecular interactions within the monolayer leading to lowering of compaction.

### 5.3 Nickel oxide films

In this work Ni-stearate LB films are deposited on a glass substrate and calcined to form Nickel Oxide. To form dense uniform films maximum incorporation of  $\text{Ni}^{2+}$  ions in the Langmuir monolayer formed on the trough is required. Also the monolayers should have sufficiently high elasticity to ensure transfer of films onto the substrates without breaking. Taking both these parameters into consideration the main set of depositions has been done at subphase pH of 7.9. To understand the effect of pH on the Nickel Oxide film morphology one set of data was also taken for different subphase pH.

#### 5.3.1 Deposition of Ni-stearate Langmuir-Blodgett films:

Figure 5.8 shows the representative graph between transfer ratio and layer number for one set of transfer. For ideal homogeneity transfer ratio should lie above 0.8 and below 1.2. From graph it is clear that there is Y-type deposition as there is deposition on both up and down strokes and the deposited layers are homogeneous.

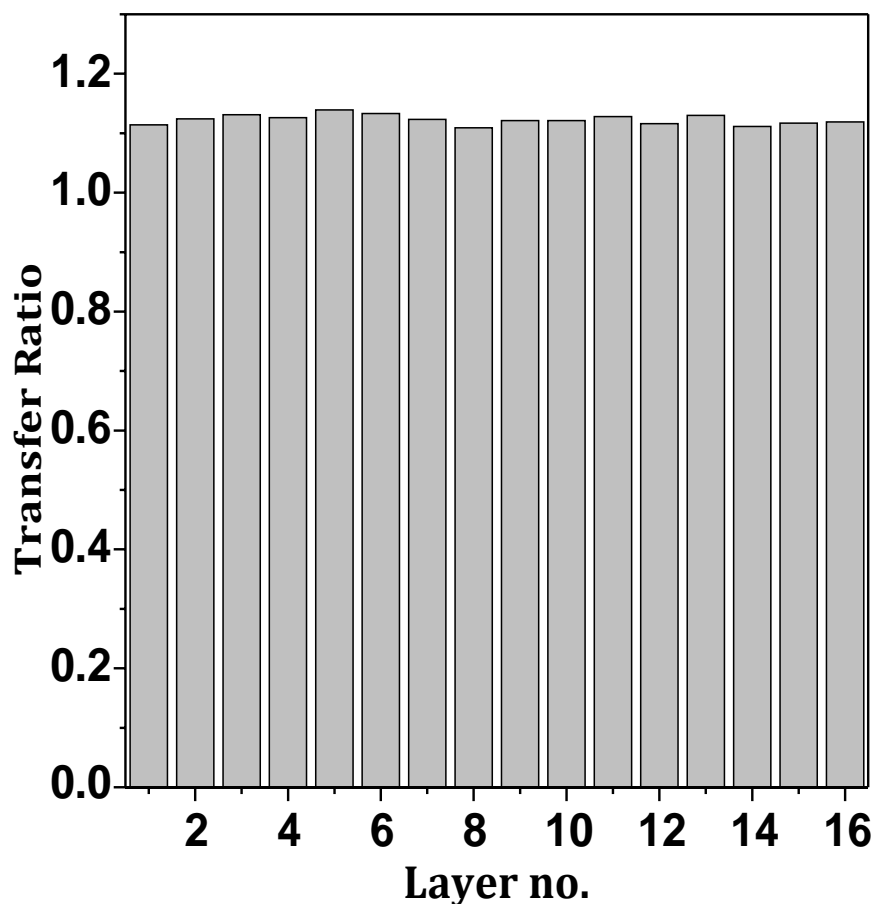
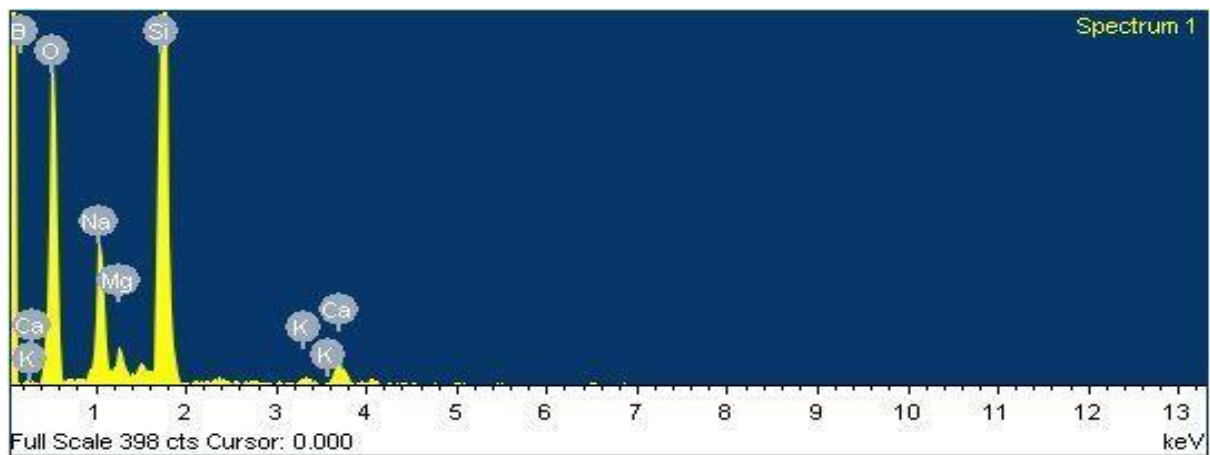


Figure 5.8: Graph between transfer ratio and layer number.

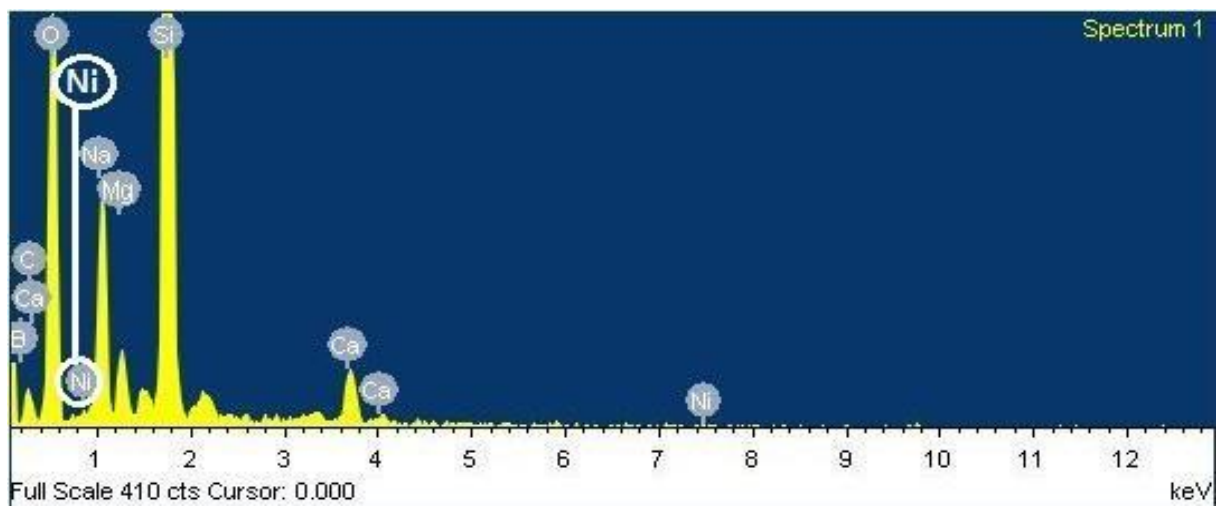
The deposited LB films were dried and calcined in high temperature furnace for the final phase formation as per the protocol discussed in section 4.2.7. The final temperatures and times are based on the literature survey [6-8].

### 5.3.2 Energy-Dispersive X-ray Spectroscopy (EDS):

To confirm the presence of Ni in the final phase formed films the EDS spectrum of the bare glass substrate was compared with one having the film. Figure 5.9 clearly confirms the presence of Ni in the annealed films.



(a)



(b)

**Figure 5.9:** EDX pattern of (a) bare glass slide (b) glass slide with phase formed film for the 79Ni19 sample.

### 5.3.3 XRD

The phase formation in the calcined films was checked using XRD. Figure 5.10 shows the XRD pattern of 79Ni15 sample after oxide phase formation. There are no distinct peaks but broad peaks are seen at  $2\theta \sim 32, 55$  and  $60$ . These match with earlier results in the group indicating that the phase formed is hexagonal  $\text{Ni}_2\text{O}_3$  (ICDD – No: 00-014-0481) [6]. Lack of distinct peaks is expected since the thickness of the films is very less. The thickness of the films was not measured but it is expected to be in the range of 5-7 nm. This number has been arrived at since for 200 layer deposition we get a film of nearly 70 nm [6].

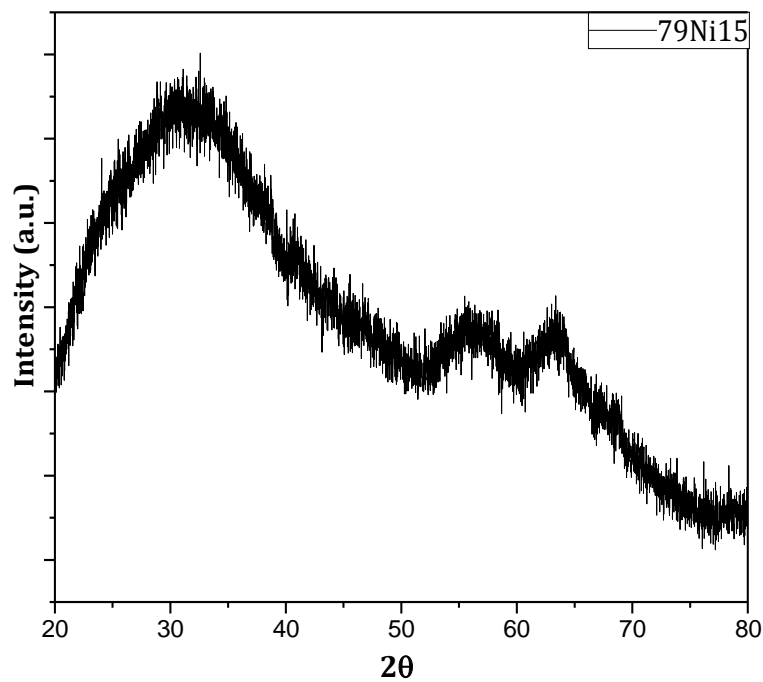


**Figure 5.10:** XRD pattern for the Nickel oxide thin film obtained from 15 layer deposition.

### 5.3.4 Ultraviolet-Visible Spectroscopy (UV-Vis):

Figure 5.11 (a) shows absorbance spectra obtained from Ultraviolet-visible spectroscopy of 79Ni19 sample. Band gap of NiO thin film calculated using Tauc plot as shown in figure 5.11 (b) is 4.0 eV. This bandgap matches the values obtained for thin films of Nickel Oxide in literature. The sample shows low absorbance which indicates crystalline nature of film.

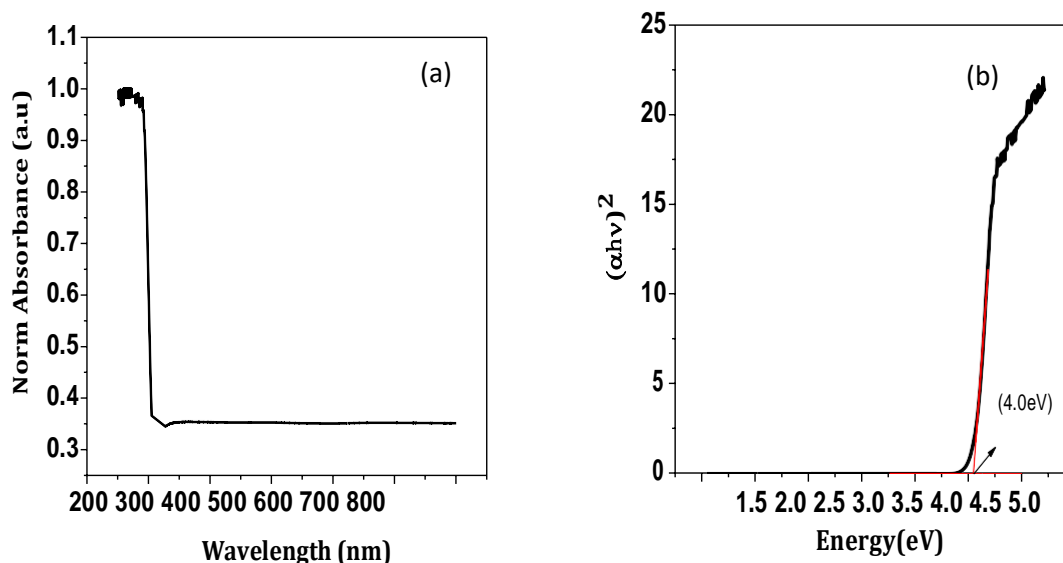


**Figure 5.11:** (a) The absorbance spectra and (b) Tauc plot for 79Ni19.

### 5.3.5 Nickel oxide thin film morphology

The surface morphology of the calcined films was characterized with FE-SEM. The images obtained were analysed using Axio Vision software and grain size distribution was determined for each sample.

#### 5.3.5.1 Effect of number of layers:

Final morphology of the Nickel Oxide films will be affected by the number of Ni-stearate layers deposited since it will decide the amount of nickel present on the surface. Figure 5.12 FE-SEM images and the respective grain size distribution for the 79Ni10, 79Ni15, 79Ni19 samples deposited at pH 7.9.

The grain size distribution analysis shows that the grain size for the oxide thin films follows Gaussian distribution. Table 5.5 gives the details of the samples and the average grain size for each sample. A close look at the SEM images shows that the 15 layer deposition gives the most uniform and continuous film. The films obtained for 10 layers have a wider distribution of grains and that for 19 layers shows enhanced granularity. So for the formation of continuous, uniform film 15 layers were deposited.

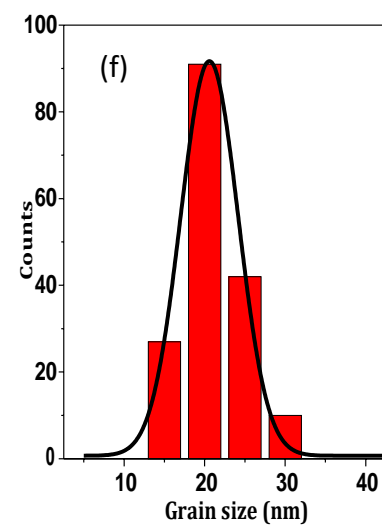
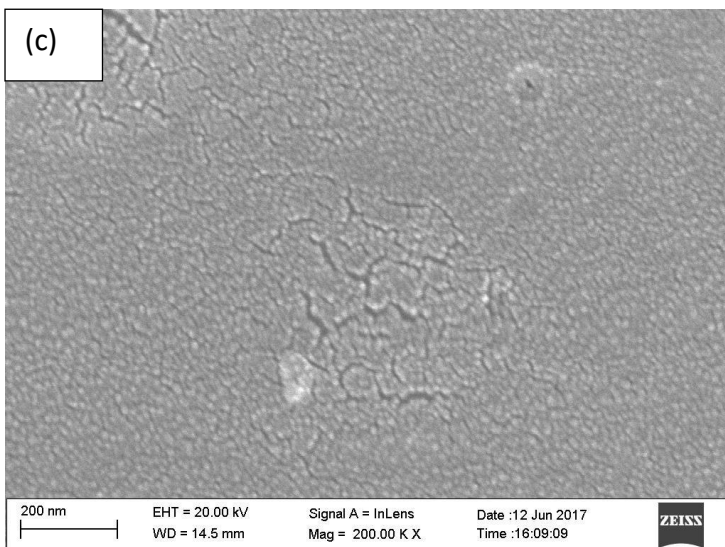
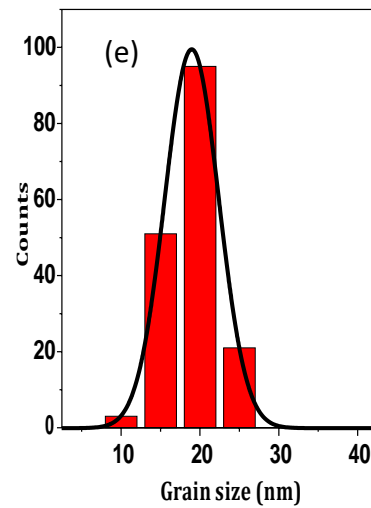
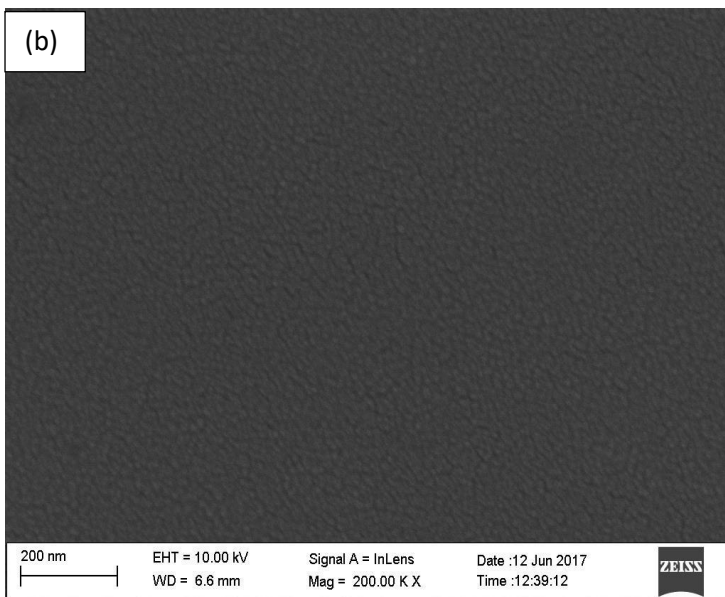
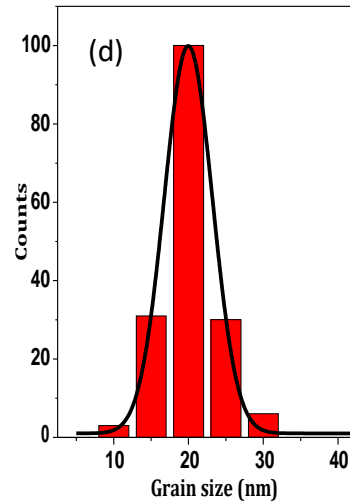
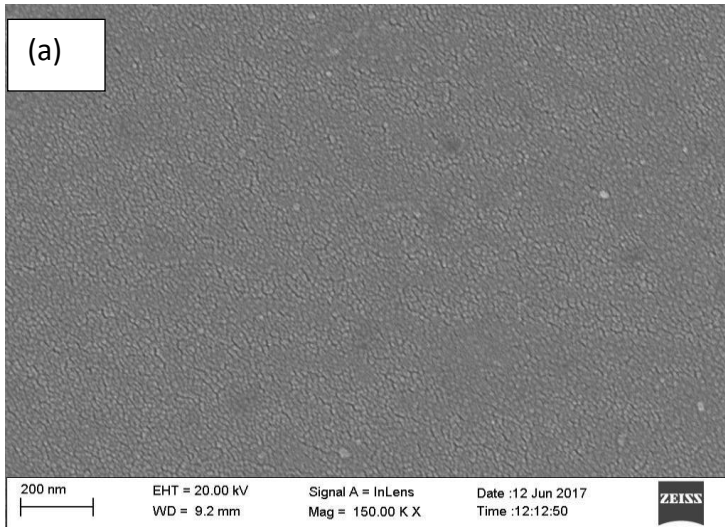


**Figure 5.12:** FE-SEM images and grain size distribution for (a, d) 79Ni10, (b, e) 79Ni15, (c, f) 79Ni19 samples.

**Table 5.5:** Sample details and average grain size of nickel oxide thin films of different thickness.

<b>Sample</b>	<b>No. of layers</b>	<b>Average grain size (nm)</b>
79Ni10	10	20
79Ni15	15	18.97
79Ni19	19	20.585

### 5.3.5.2 Effect of subphase pH:

pH effects the incorporation of nickel as well as the layer compaction of the Nickel-stearate monolayers. Both these factors affect the distribution of Nickel and hence the morphology of the final films. To understand the effect of pH on the morphology LB films were deposited with different subphase pH. The number of layers transferred for this was fixed as 15 since continuous homogenous film was obtained for pH 7.9. Figure 5.13 FE-SEM images and the respective grain size distribution for the 69Ni15, 79Ni15, and 83Ni15 samples. The grain size distribution analysis shows that the grain size for the oxide thin films follows Gaussian distribution. Table 5.6 gives the details of the samples and the average grain size for each sample. FE-SEM images clearly show that for pH 6.9 and 8.3 the final films are non-continuous and have large grain size distribution. This result further supports our earlier conjectures that at low pH we have too small amount of Ni<sup>2+</sup> ion incorporation whereas for 8.3 pH the decreased interactions leads to decompaction of the film resulting in Ni being spread all over the sample in a non-uniform way.

**Table 5.6:** Sample details and average grain size of nickel oxide thin films deposited at different pH.

<b>Sample</b>	<b>pH</b>	<b>Average grain size (nm)</b>
69Ni15	6.9	25.98
79Ni15	7.9	18.97
83Ni15	8.3	25

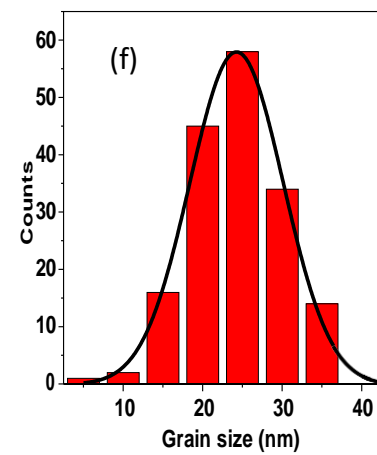
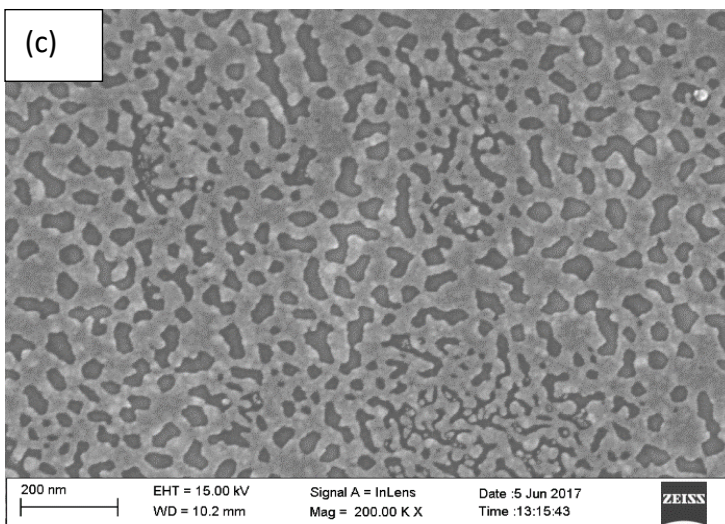
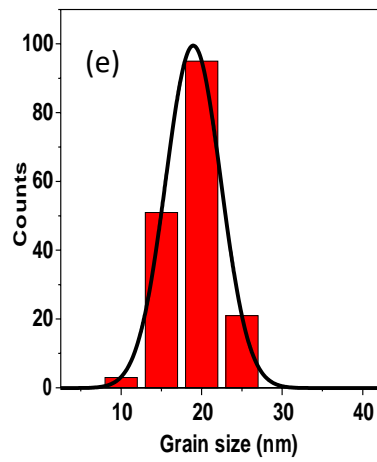
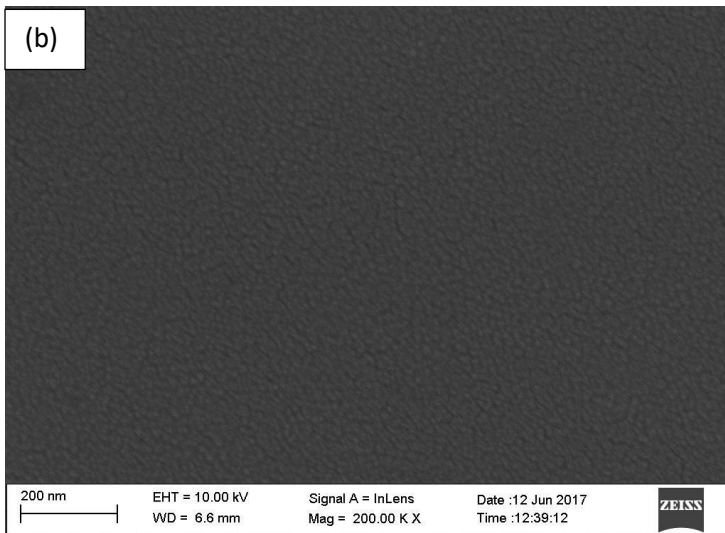
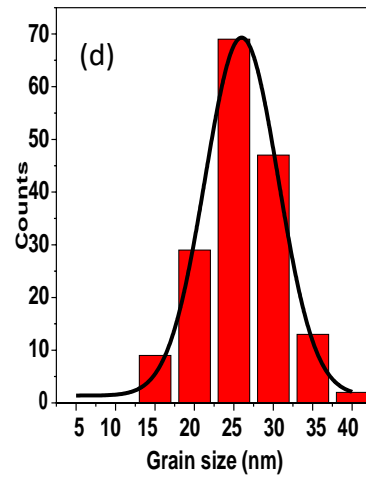
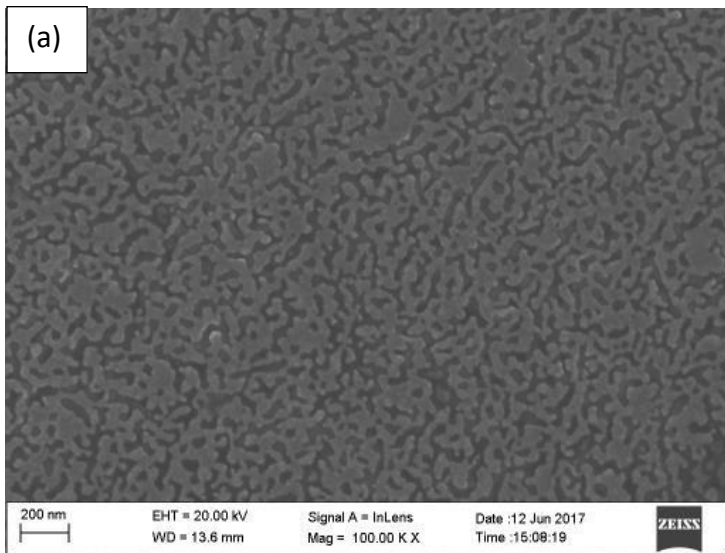


**Figure 5.13:** FE-SEM images and grain size distribution for (a, d) 69Ni15, (b, e) 79Ni15, (c, f) 83Ni15.

## 5.4 References:

1. J.B.Peng, G.T.Barnes, I.R.Gentle, *Advances in colloidal and interface science*, 91(2001), 163-219.
2. Elizabeth C. Griffith, Teobaldo R. C. Guizado, André S Pimentel, *J. Phys. Chem*, 117 (2013), 22341–22350.
3. E.A.Silva, V.J.R.Oliveira, M.L.Braunger, C.J.L.Constantino, C.A.Olivati, *Materials Research*, 1590(2014), 1516-1439.
4. S.Sudheesh, J.Ahmad, G.S.Singh, *ISRN Physical Chemistry*, 2012 (2012),835397.
5. R.Kaur, G.K.Bhullar, K. K. Raina, *AIP Conference Proceedings*, 1377(2013), 1536.
6. Palvi, P.Sharma(Guide), L.K.Brar(Guide), *Masters Theses@SPMS*, TuDR, (2016).
7. S.Sharma, M.Kumar, S.Rani, D.Kumar, C.C. Tripathi, *The Minerals, Metals & Materials Society and ASM International 2015*, 46A(2015), 3166.
8. M.Jlassi, I.Sta, M.Hajji, H.Ezzaouia, *Materials Science in Semiconductor Processing*, 21(2014), 7–13.

## Conclusions and Future Scope

---

### 6.1 Conclusions

In this work the thin uniform films of nickel oxide were synthesized from the Ni-stearate LB films. Stable and compact Langmuir monolayers are the first step in LB film deposition. Their characteristics decide the quality of LB films and the morphology of the final phase formation. Ni-stearate Langmuir monolayers were deposited and characterized on the surface of the Langmuir trough. It was observed that as the concentration and pH of subphase increased the compaction of the film and its static elasticity in the solid phase increased indicating an increase in Ni<sup>2+</sup> ion incorporation. An important result to emerge from these studies was that for very high pH (8.3) the structure of the films opens up. Analysis of  $\pi$ -A isotherms indicated that pH 7.9 had good parameters for the LB deposition. The oscillating barrier characterizations of Ni stearate monolayers at different frequencies and pH values were recorded. It also confirmed the stability of the monolayers at pH 7.9. Transparent Nickel oxide thin films on glass substrate were synthesized by deposition of 10, 15, 19 layers of Ni-stearate at 7.9 pH followed by drying, removal of stearate chain and calcination. The presence of Ni in thin films was checked by EDS. The synthesized nickel oxide thin film has the band gap of 4.04 eV. The thin films formed by deposition of 15 layers of nickel stearate deposited at pH 7.9 were continuous and uniform. The effect of pH on the final film morphology was determined by depositing 15 layers of Ni stearate for 6.9 and 8.3 pH values. The results showed that these films are non-continuous and have large grain size distribution.

### 6.2 Future Scope

The Nickel oxide thin films should be characterized topographically and analysed for roughness. This is important especially for layered device applications such as photo voltaic and smart window applications. The relaxation process signals emerging in oscillatory barrier experiments need to be explored further to understand the underlying phenomena occurring in these Langmuir monolayers.

